

*Full Length Research Paper*

# Performance characteristics of high speed laser diodes under thermal-irradiated operating conditions

**Abd El-Naser A. Mohammed, Mohamed M. S. El-Halawany, Gaber E. M. El-Abyad and Mohammed S. F. Tabbour\***

Department of Electronic and Electrical Communication Engineering, Faculty of Electronic Engineering, Menouf, 32951, Menoufia University, Egypt.

Accepted 13 November, 2009

**In the present paper, under thermal-irradiated operating conditions, the performance characteristics of high speed laser diodes (based on Vertical Cavity Surface Emitting Laser (VCSELs)) are deeply and parametrically investigated. The processed characteristics are: the harmonic response transfer function, the resonance frequency, 3-dB bandwidth and the rise time. These diodes affect the transmitted bit-rate in high-speed advanced optical communication systems. The effects of both ambient temperature (and consequently the inner temperature), the injected current (power) and the dose of irradiation are deeply investigated. The pulse rise time and the resonance frequency as well as the 3-dB bandwidth are the major criterions of the device speed. Nonlinear relations are correlated to investigate the power-current and the voltage-current dependences of the devices. Although a considerable amount of radiation effects studies on individual devices exposed to a variety of radiation conditions is reported in literature, only little information is available on the radiation tolerance at high total dose ( $> 1$  MGy) and under neutron radiation.**

**Key words:** VCSEL, performance characteristics, radiation.

## INTRODUCTION

In recent years, a new type of semiconductor laser has attracted considerable interest, namely, the vertical-cavity surface-emitting laser (VCSEL). VCSELs compose the most suited laser configuration for the fiber application and they are of a special impact in the field of optical interconnection (Piskorski et al., 2008; Ortiz et al., 1997; Ortiz et al., 1996). This device offers many advantages over edge-emitters, resulting in its growing popularity in the field of optoelectronics, including single-longitudinal-mode operation, circular output beams, suitability for monolithic two-dimensional integration and compatibility with on-wafer probe testing (Iga et al., 1988).

Radiation-induced failures of these devices have been observed in the optical networks in space and have been further documented at similar radiation doses in the laboratory. Thus, it will be important for the space com-

munity to have access to radiation hardened/tolerant optics. For many microelectronic and photonic devices, it is difficult to achieve radiation hardness without sacrificing performance. However, in the case of optocouplers, one should be able to achieve both superior radiation hardness and performance for such characteristics as switching speed, current transfer ratio (CTR), minimum power usage and array power transfer, if standard light emitting diodes (LEDs), such as those in the commercial optocouplers mentioned above, are avoided and VCSELs are employed as the emitter portion of the optocoupler. For VCSEL-based optocouplers to be broadly applicable to a variety of space missions, the radiation hardness of these devices must be sufficient to survive a variety of radiation environments from Low Earth Orbit (LEO) to Galactic Cosmic Rays (GCR) to Mars missions to the stringent requirements of a Jupiter - Europa mission. Near the laser threshold current, the losses experienced by the light beam as it traverses the optical laser cavity are equal to the optical gains due to stimulated emission. Thus, if the rate of non-radiative recombination is increas-

\*Corresponding author. E-mail: mohsaltab@yahoo.com.

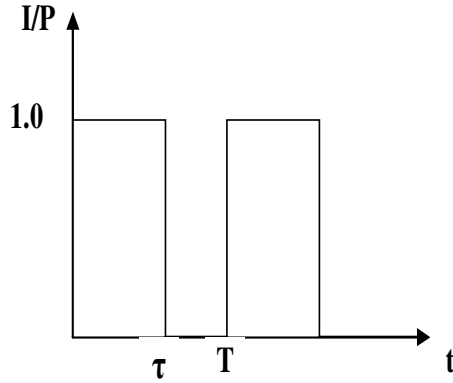
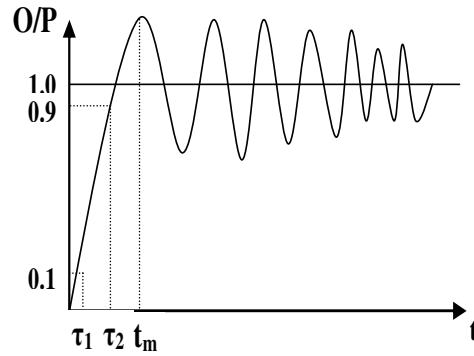


Figure 1. Input / Output of optical source.



ed due to irradiation, the cavity losses will increase and the threshold current will increase correspondingly. In addition, heating effects due to increased total current flow will adversely affect VCSEL operation at high currents well into lasing. While some work has been done on radiation effects in VCSELs, the efforts to date are not extensive enough to provide a complete radiation hardness assurance (RHA) description, particularly for oxide-confined VCSELs (Constantinescu et al., 2002; Barnes et al., 2000).

The radiation is expected to cause atomic displacement damage by nuclear interactions. The defects can act as non-radiative recombination centers, which decreases the minority carrier lifetime and results to increase in laser threshold current. However, most of this damage can be removed by injection annealing (Chu et al., 2007; Teny et al., 2003). Due to their poor heat dissipation and the large resistance introduced by their distributed Bragg reflectors (DBRs), typical VCSELs undergo relatively severe heating and consequently can exhibit strong thermally dependent behavior (Tabbour, 2005). In the present paper, the harmonic response characteristics of VCSEL (Thin oxide aperture operates at 850 nm) will be deeply and parametrically studied in thermo-irradiated field (TIF). Special emphasis is given to: the magnitude of the harmonic transfer function, the device 3-dB bandwidth, the resonance frequency, the damping frequency and rise time. Severe radiation or thermal or both penalties have been modeled and investigated, where the third case possesses double impact in reducing the device bandwidth. It is found that the device undergoes the ultimate relative reduction, while the device is of the minimum relative reduction. The data and results given in the present paper are a set of samples for the device.

**BASIC MODEL AND ANALYSES**

Based on Tabbour (2005), Mena et al. (1999a; b) and Carroll et al. (1998), the magnitude of the normalized harmonic response of VCSEL in the S-domain is given by:

$$G_n(s) = \frac{\omega_n^2}{S^2 - BS + \omega_n^2} \tag{1}$$

Where,

$\omega_n$  is the device natural frequency, B is the damping coefficient, and S is due to Laplace transform.

$G_n(s)$  can be modified as:

$$G_n(s) = \frac{\omega_n^2}{(S - B/2)^2 + \omega_n^2 - B^2/4} = \frac{\omega_n^2}{(S - B/2)^2 + \omega_d^2} \tag{2}$$

Thus, for the narrow square pulse shown below in Figure 1.

$$g_n(t) = [1.0 - (A_m e^{-Bt/2}) \sin \omega_d t]u(t) - [1.0 - (A_m e^{-B(t-\tau)/2}) \sin \omega_d (t - \tau)]u(t - \tau) \tag{3}$$

With  $\omega_d = \sqrt{\omega_n^2 - 0.25 B^2}$  and  $A_m = \omega_n/\omega_d$

One normalized electric bit of duration T and pulse width  $\tau$  and its optical output power are shown above. Both  $\tau_2$  and  $\tau_1$  are the solutions of

$$g_n(\tau_2) = 0.9 \tag{4}$$

$$g_n(\tau) = 0.1 \tag{5}$$

A special software is designed to handle both Equations (4) and (5) to find both  $\tau_2$  and  $\tau_1$  and consequently the rise time  $\tau_r$  where:

$$\tau_r = \tau_1 - \tau_2 \tag{6}$$

An important application in high-speed optical interconnection in thermo-irradiated field is the effect of both the temperature T and the irradiation dose D. Based on the investigation of Mena et al. (1999a,1999b), we derive the following: The resonance frequency  $\omega_r$ , the 3-dB bandwidth  $\omega_{3-dB}$ , the maximum overshoot  $G_m$  and the maximum time response  $g_{mt}$ , are obtained as:

a)  $\omega_r$  is  $\omega$  at which  $dG_n/d\omega = 0.0$  which yields:

**Table 1.** Coefficients of Equations 13, 14 and 18.

$\alpha_{i,s}$	$\beta_{i,s}$	$\gamma_{i,s}$	$\nu_{i,s}$
$0.4807 \times 10^{-3}$	$0.2294 \times 10^{-1}$	$0.2294 \times 10^{-1}$	2.937
$-0.1095 \times 10^{-2}$	$0.5413 \times 10^{-2}$	$-0.1095 \ 0.2294 \times 10^{-2}$	-1.07
$-0.7922 \times 10^{-4}$	$-0.2877 \times 10^{-3}$	$-0.2877 \ 0.2294 \times 10^{-3}$	0.1815
$0.2797 \times 10^{-5}$	$0.4705 \times 10^{-5}$	$0.4705 \ 0.2294 \times 10^{-5}$	-0.011

$$\omega_r = \sqrt{\omega_n^2 - 0.5B^2} = 2\pi f_r \quad (7)$$

b)  $\omega_{3-dB}$  is  $\omega$  at which  $|G_n(\omega)| = 0.5$  which yields:

$$\omega_{3-dB} = \omega_r \sqrt{1 + \sqrt{1 + 3(\omega_n^2 / \omega_r^2)^2}} = 2\pi f_{3-dB} \quad (8)$$

The Power-Forward Current-Voltage (P-I-V) curves of 4 types of VCSELs were given in Mena et al. (1999a, 1999b), with remarkable nonlinearly while in Berghmans et al. (2002) it depicted in linear fashion. Based on the data of Mena et al. (1999a, 1999b), the following nonlinear thermal relations for the set of the selected device were carried out:

$$P(I, T) = p_0 + p_1 I + p_2 I^2 + p_3 I^3 + p_4 I^4, \text{ mW} \quad (9)$$

$$v(I, T) = v_0(T) + v_1 I + v_2 I^2 + v_3 I^3, \text{ V} \quad (10)$$

Where the elements of the set  $\{p_0, p_1, p_2, p_3, p_4, v_0\}$  are polynomial functions of T.

$$p_0 = 0.7262 - 0.1696 \times 10^{-2} T + 0.3452 \times 10^{-4} T^2 - 0.703 \times 10^{-7} T^3$$

$$p_1 = 2.463 + 0.7106 \times 10^{-2} T - 0.1097 \times 10^{-3} T^2 + 0.2058 \times 10^{-6} T^3$$

$$p_2 = -7.2847 - 0.2006 \times 10^{-2} T + 0.6046 \times 10^{-4} T^2 - 0.1252 \times 10^{-6} T^3$$

$$p_3 = 0.23483 + 0.49794 \times 10^{-3} T - 0.1135 \times 10^{-4} T^2 + 0.2240 \times 10^{-7} T^3$$

$$p_4 = -0.91743 \times 10^{-2} - 0.2908 \times 10^{-4} T + 0.451 \times 10^{-6} T^2 - 0.79164 \times 10^{-9} T^3$$

$$v_0 = 0.5718 - 1.64 \times 10^{-4} (T - 300)$$

Where the set of coefficients  $\{v_1, v_2, v_3\}$  is shown in Table 1. The irradiation effect is computed based on the results of Tabbour (2005) and Mena et al. (1999a, 1999b), we cast:

$$P(I, T, D) = P(I, T) F_p(D) \quad (11)$$

$$V(I, T, D) = V(I, T) F_v(D) \quad (12)$$

Where both  $F_p(D)$  and  $F_v(D)$  are functions of the dose of irradiation, D

$$F_p(D) = 1 + \alpha_1 D + \alpha_2 D^2 + \alpha_3 D^3 + \alpha_4 D^4 \quad (13)$$

$$F_v(D) = 1 + \beta_1 D + \beta_2 D^2 + \beta_3 D^3 + \beta_4 D^4 \quad (14)$$

Where the sets of coefficients are given in Table 1. The minority and majority carrier lifetimes  $\tau_{p,n}$  under irradiation is given by Teny et al. (2003), Tabbour, (2005), Mena et al. (1999a, 1999b), Carroll et al. (1998) and Berghmans et al. (2002):

$$\frac{1}{\tau_{np}} = \frac{1}{\tau_{onp}} + k\phi \quad (15)$$

Where  $\tau_{onp}$  denotes the pre-irradiation minority carrier lifetime, k is a damage constant, and  $\phi$  is the fluence,  $\text{cm}^2$ . In the present analysis, we consider that:

$$k / \tau_{onp} = 6 \times 10^{-6} \text{ cm}^2/\text{sec}, \text{ thus} \quad (16)$$

$$\tau_{np} = \tau_{onp} (1 + \tau_{onp} k\phi)^{-1} \quad (17)$$

Based on the data published by Berghmans et al. (2002, 2002a, 2000b), we recast the offset current  $I_{off}(T)$  under irradiation under the form:

$$I_{off}(T, D) = I_{off}(T) (\gamma_0 + \gamma_1 D + \gamma_2 D^2 + \gamma_3 D^3 + \gamma_4 D^4) \quad (18)$$

Where  $\gamma_0, \gamma_1, \gamma_2, \gamma_3,$  and  $\gamma_4$  are constant coefficients given in Table 1.

## RESULTS AND DISCUSSION

The thermo-Irradiated Field (TIF) is assumed under the following ranges of causes (affecting parameters),  $(0.0 \leq D \text{ fluence}/10^{14} \leq 25.0) \text{ n/cm}^2$ ,  $(300.0 \leq T \leq 320.0) \text{ K}$ ,  $(1.0 \leq I \leq 6.0) \text{ mA}$ .

It is necessary to stress that the major generator of features is the fluence due to the damage which causes dislocations; and radiation-induced defects is the band gap. Based on the above model of TIF, variations of set of five causes  $\{f_{BW}, f_R, f_d, G_{max}$  and  $\tau_r\}$  against variations of a set of three effects  $\{D, T, I\}$  are displayed in Figures 2 - 9. As shown in Figures 2, 3, 4, 6 and 7, the 3-dB bandwidth, the resonance frequency and damping frequency decrease as the damage caused by the fluence D

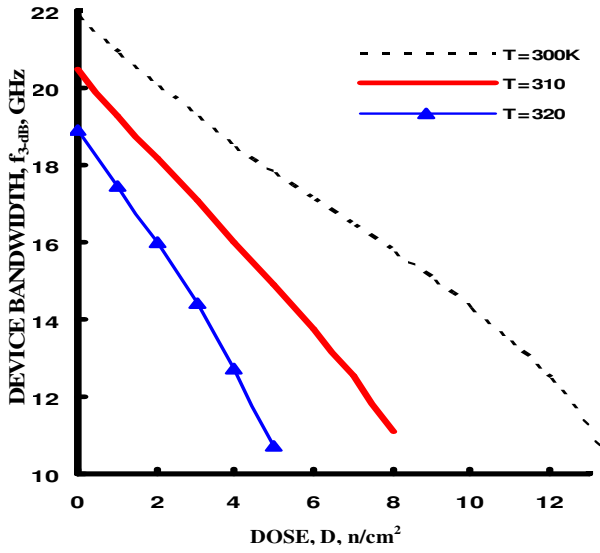


**Figure 2.** Variations of device bandwidth,  $f_{3-dB}$ , GHz against variations of dose  $D$ ,  $n/cm^2$  at the other set of parameters.  $T_o = 290$  K,  $I = 2$  mA,  $\lambda_s = 850$  nm,  $p_{so} = 1$  mW,  $\Delta n = 0.0075$ ,  $\Delta \lambda = 0.5$  mm,  $g_o = 0.8486 \times 10^6$ ,  $R_{th} = 0.89$ ,  $N_o = 0.1286 \times 10^7$ .

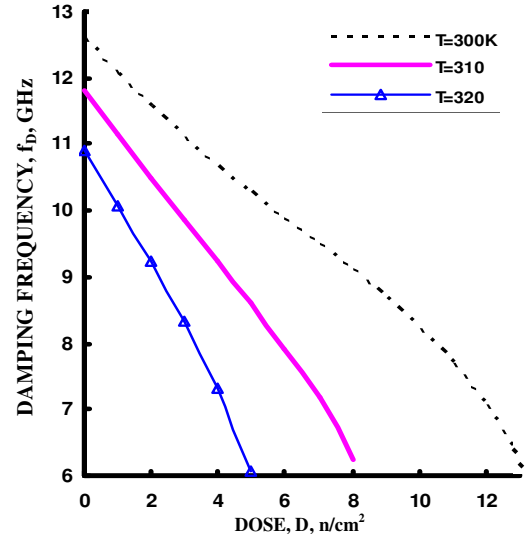


**Figure 4.** Variations of damping frequency,  $f_d$ , GHz against variations of dose  $D$ ,  $n/cm^2$  at the other set of parameters.  $T_o = 290$  K,  $I = 2$  mA,  $\lambda_s = 850$  nm,  $p_{so} = 1$  mW,  $\Delta n = 0.0075$ ,  $\Delta \lambda = 0.5$  mm,  $g_o = 0.8486 \times 10^6$ ,  $R_{th} = 0.89$ ,  $N_o = 0.1286 \times 10^7$ .

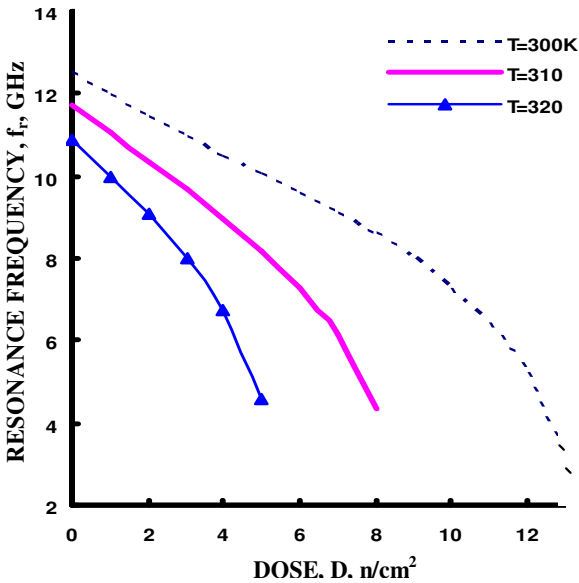


**Figure 3.** Variations of resonance frequency,  $f_r$ , GHz against variations of dose  $D$ ,  $n/cm^2$  at the other set of parameters.  $T_o = 290$  K,  $I = 2$  mA,  $\lambda_s = 850$  nm,  $p_{so} = 1$  mW,  $\Delta n = 0.0075$ ,  $\Delta \lambda = 0.5$  mm,  $g_o = 0.8486 \times 10^6$ ,  $R_{th} = 0.89$ ,  $N_o = 0.1286 \times 10^7$ .

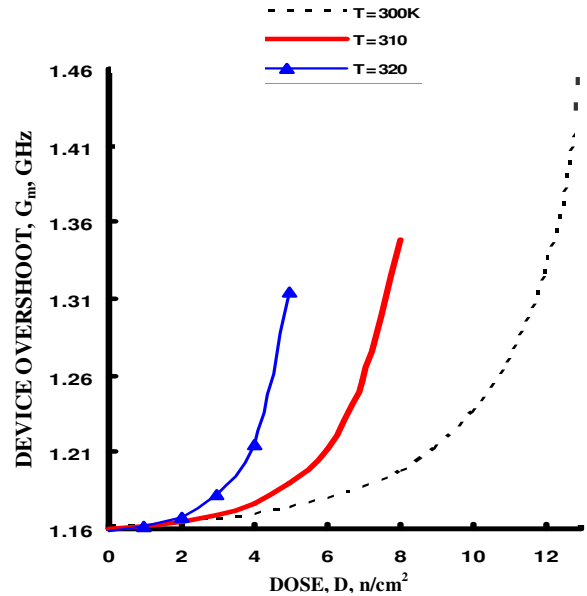


**Figure 5.** Variations of device overshoot,  $G_m$ , GHz against variations of dose  $D$ ,  $n/cm^2$  at the other set of parameters.  $T_o = 290$  K,  $I = 2$  mA,  $\lambda_s = 850$  nm,  $p_{so} = 1$  mW,  $\Delta n = 0.0075$ ,  $\Delta \lambda = 0.5$  mm,  $g_o = 0.8486 \times 10^6$ ,  $R_{th} = 0.89$ ,  $N_o = 0.1286 \times 10^7$ .

increases, or as the ambient temperature increases, while they increase as the injection current increases. On contrary, as shown in Figures 8 and 9, the rise time increases as the damage caused by the fluence increases, or as the ambient temperature increases, while they decreases as the injection current increases. Finally, as shown in Figure 5, the device overshoot increases as the

damage caused by the fluence increases, or as the ambient temperature increases.

**Conclusion**

The response of VCSEL optical source in Thermo-

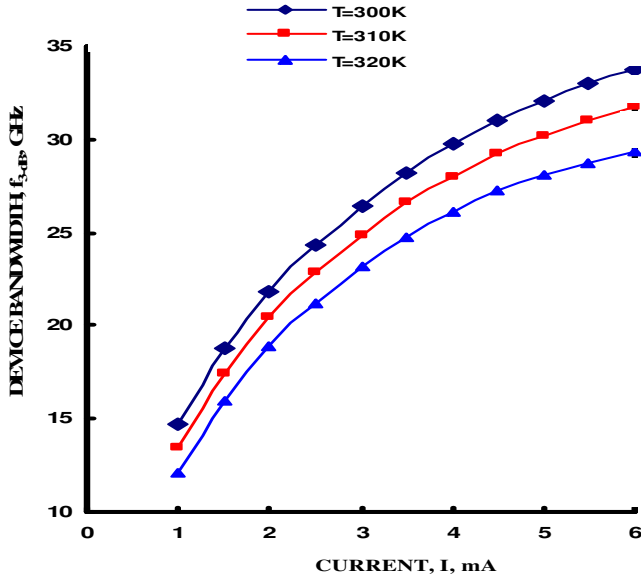


**Figure 6.** Variations of device bandwidth,  $f_{3-dB}$ , GHz against variations of current  $I$ , mA at the other set of parameters.  $T_o = 290$  K $^\circ$ ,  $D = 0$  n/cm $^2$ ,  $\lambda_s = 850$  nm,  $p_{so} = 1$  mW,  $\Delta n = 0.0075$ ,  $\Delta \lambda = 0.5$  mm,  $g_o = 0.8486 \times 10^6$ ,  $R_{th} = 0.896$ ,  $N_o = 0.1286 \times 10^7$ .

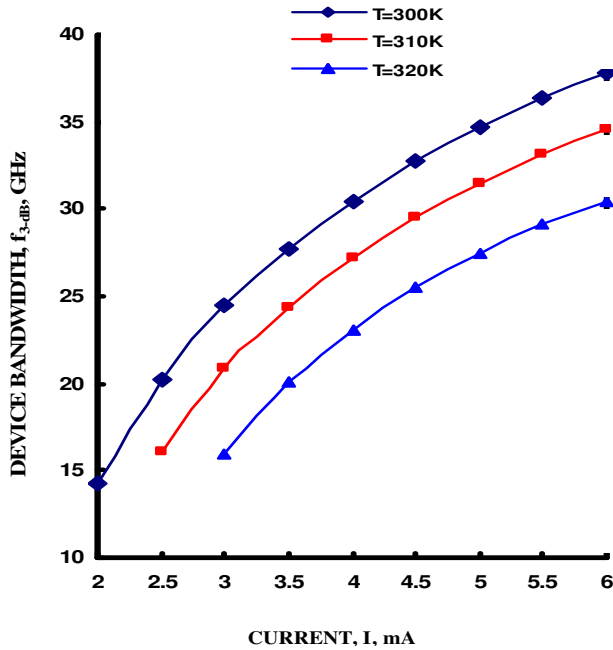


**Figure 7.** Variations of device bandwidth,  $f_{3-dB}$ , GHz against variations of current  $I$ , mA at the other set of parameters.  $T_o = 290$  K $^\circ$ ,  $D = 10$  n/cm $^2$ ,  $\lambda_s = 850$  nm,  $p_{so} = 1$  mW,  $\Delta n = 0.0075$ ,  $\Delta \lambda = 0.5$  mm,  $g_o = 0.8486 \times 10^6$ ,  $R_{th} = 0.896$ ,  $N_o = 0.1286 \times 10^7$ .

Irradiated Field (TIF) is modeled and investigated under wide ranges of affecting parameters (causes) through the generalized harmonic transfer function. The following conclusions are clarified: i). The damage caused by the

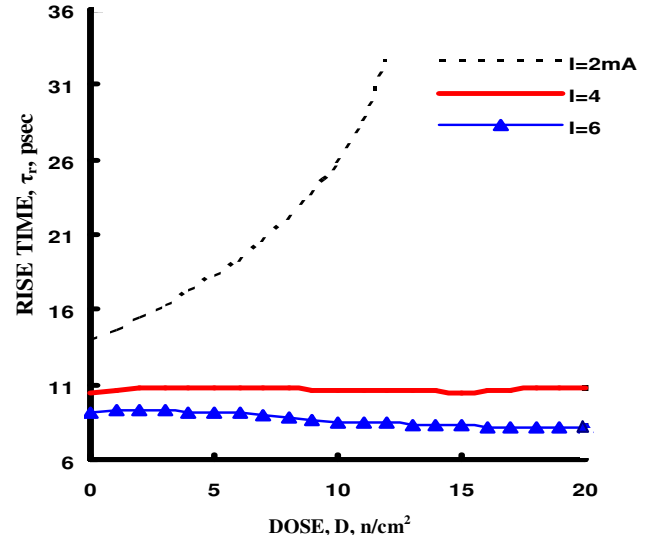


**Figure 8.** Variations of  $\tau_r$ , psec against variations of doses  $D$ , n/cm $^2$  at the other set of parameters.  $T_o = 290$  K $^\circ$ ,  $T = 300$  K $^\circ$ ,  $\lambda_s = 850$  nm,  $p_{so} = 1$  mW,  $\Delta n = 0.0075$ ,  $\Delta \lambda = 0.5$  mm,  $g_o = 0.8486 \times 10^6$ ,  $R_{th} = 0.896$ ,  $N_o = 0.1286 \times 10^7$ .

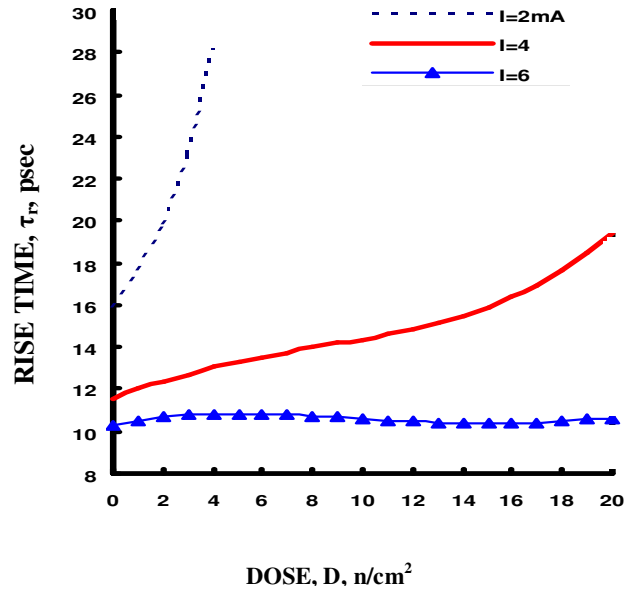


**Figure 9.** Variations of  $\tau_r$ , psec against variations of doses  $D$ , n/cm $^2$  at the other set of parameters.  $T_o = 290$  K $^\circ$ ,  $T = 320$  K $^\circ$ ,  $\lambda_s = 850$  nm,  $p_{so} = 1$  mW,  $\Delta n = 0.0075$ ,  $\Delta \lambda = 0.5$  mm,  $g_o = 0.8486 \times 10^6$ ,  $R_{th} = 0.896$ ,  $N_o = 0.1286 \times 10^7$ .

fluence  $D$ , decreases  $f_{3-dB}$ ,  $f_r$  and  $f_d$  whatever the set of effects  $\{T, I\}$ ; ii) The damage caused by the fluence  $D$ , increases  $\tau_r$  whatever the set of effects; iii) At any set of causes  $\{T, I, D\}$ ,  $f_{3-dB} > f_r > f_d$ ; iv) The speed of the device is, in general, in nonlinear positive correlation with the current and is in nonlinear negatives correlation with either  $D$  or  $T$  or both, and; v) The breakdown of the de-

vice (full damage that is the stopping of action) is caused when current  $I \ll 1$  mA and at temperature  $T > 320$  K and  $D > 25.0$  and finally the device is more stable at higher currents.

## REFERENCES

- Barnes CE, Schwank JR, Swift GM, Armendariz MG, Johnston A, Guertin S, Hash GL, Choquette KD (2000). "Proton Irradiation Effects in Oxide-Confined Vertical Cavity Surface Emitting Laser (VCSEL) Diodes", RADECS, Belgium.
- Berghmans F (2000). "Radiation Effects in Optical Communication Devices," Proc. Symp. IEEE/LEOS Benelux Delft Netherland. p. 63.
- Berghmans F, Uffelen MV, Decreton M (2002). "Combined Gamma and Neutron Radiation Effects on VCSELs, Proc. Sym. IEEE/LEOS Benelux Chapter, Amsterdam. pp. 71-79.
- Berghmans F, Uffelen MV, Decreton M (2002). "High Total Dose Gamma and Neutron Radiation Tolerance of VCSEL Assemblies," SPIE Proc., Conf. Photonics for Space Environments V111, <http://WWW.tona.vub.ac.be>. 4823: 23.
- Carroll J, Whiteaway J, Plumb D (1998). Distributed Feedback Semiconductor Lasers, Ch.8, IEE Redwood Books, Trowbridge.
- Chu ML, Hou S, Huffman T, Issever C, Lee SC, Lu RS, Su DS, Teng PK, Weidberg AR (2007). "Radiation hardness studies of VCSELs and PINs for the opto-links of the Atlas Semiconductor Tracker", Elsevier J. Nuclear Ins. S. Meth.s Phy.Res. A579: 795-800.
- Constantinescu B, Nicolescu C, Teodorescu C, Constantin F, Bugoi R, Ioan P, Radulescu L, Brasoveanu M, Dragusin M (2002). "Gamma and Proton Irradiation Effects on Optical Transmission Materials for Plasma Diagnostics Innuclear Fusion Reactor", 29th EPS Conference on Plasma Phys. and Contr. Fusion Montreux 26B: 17-21.
- Iga K, Koyama F, Kinoshita S (1988). "Surface – Emitting Semiconductor Lasers", IEEE J. Quantum Electron 24(9): 1845–1855.
- Mena PV, Morikuni JJ, Kang SM, Harton AV, Wyatt KW (1999). "A Simple Rate-Equation-Based Thermal VCSEL Model," J. Lightwave Technol. 17(5): 865-872.
- Mena PV, Morikuni JJ, Kang SM, Harton AV, Wyatt KW (1999). "A Comprehensive Circuit-Level Model of Vertical-Cavity Surface-Emitting Lasers," J. Lightwave Technol. 17(12): 2612-2632.
- Ortiz GG (1996). "Monolithic, Integration of InGaAs VCSELs with Resonance – Enhanced Quantum-Well Photodetectors", Electron. Lett. 32(13): 1205-1207.
- Ortiz GG (1997). "Monolithic, Multiwavelength VCSEL Arrays by Surface-Controlled MOCVD Growth Rate Enhancement and Reduction", IEEE Photonics Technol. Lett. 8: 9.
- Piskorski L, Sarzala RP, Nakwaski W (2008). "Analysis of Anticipated performance of 650-nm GaInP/AlGaInP quantum-well GaAs-based VCSELs at Elevated temperature", Opto-Electron. Rev. 16(1): 34-41.
- Tabbour MS (2005). Sources in Optical Communications Systems, M. Sc. Thesis, Fac. Elect. Eng., Menouf, EGYPT. Pp.62-70.
- Teny PK (2003). "Radiation Hardness and Lifetime Studies of the VCSELs for the ATLAS Semiconductor Tracker," Nuclear Instruments and Method in Physics Researches A497: 294-304.